

Loss of the oligosaccharyl transferase subunit *TUSC3* promotes proliferation and migration of ovarian cancer cells

PETR VAŇHARA^{1*}, PETER HORAK^{2*}, DIETMAR PILS³, MARIAM ANEES², MICHAELA PETZ²,
WOLFGANG GREGOR⁴, ROBERT ZEILLINGER³ and MICHAEL KRAINER²

¹Department of Histology and Embryology, Faculty of Medicine, Masaryk University, Brno, Czech Republic; Departments of ²Internal Medicine I and Comprehensive Cancer Center and ³Obstetrics and Gynecology, Division of Gynecology, Medical University of Vienna; ⁴Research Group of Molecular Pharmacology and Toxicology, University of Veterinary Medicine Vienna, Vienna, Austria

Received November 18, 2012; Accepted January 8, 2013

DOI: 10.3892/ijo.2013.1824

Abstract. Consequences of deregulated protein N-glycosylation on cancer pathogenesis are poorly understood. *TUSC3* is a gene with a putative function in N-glycosylation, located on the short arm of chromosome 8. This is a chromosomal region of frequent genetic loss in ovarian cancer. We established recently that the expression of *TUSC3* is epigenetically decreased in epithelial ovarian cancer compared to benign controls and provides prognostic information on patient survival. Therefore, we analyzed the consequences of silenced *TUSC3* expression on proliferation, invasion and migration of ovarian cell lines. In addition, we performed subcellular fractionation, co-immunofluorescence and co-immunoprecipitation experiments to establish the molecular localization of *TUSC3* in ovarian cancer cells. We demonstrated that *TUSC3* is localized in the endoplasmic reticulum as a subunit of the oligosaccharyltransferase complex and is capable of modulation of glycosylation patterning of ovarian cancer cells. Most importantly, silencing of *TUSC3* enhances proliferation and migration of ovarian cancer cells *in vitro*. Our observations suggest a role for N-glycosylating events in ovarian cancer pathogenesis in general, and identify *TUSC3* as a tumor suppressor gene in ovarian cancer in particular.

Introduction

Epithelial ovarian cancer is the most lethal gynecologic malignancy and the fourth most frequent cause of cancer mortality in women in western industrialized countries (1). Early

detection and diagnosis of ovarian cancer presents one of the challenges of this entity and consequently a majority of cases are diagnosed in advanced stages (FIGO III and IV). The prognosis for women with advanced ovarian cancer remains bleak despite the advances of surgical and medical therapies in the last decades. A better understanding of the pathogenesis of ovarian cancer may lead to earlier diagnosis and novel therapies for this disease.

Tumor suppressor candidate 3 (*TUSC3*), originally named N33, was identified as a potential tumor suppressor gene in prostate cancer located on chromosome band 8p22 (2,3). Homozygous deletions of this chromosomal region have been detected in pancreatic (4,5) and prostate cancer cell lines (6,7), even though mutations of the *TUSC3* coding sequence are rare. Using a systematical screening approach, we recognized *TUSC3* as a significantly downregulated gene in ovarian cancer (8). Recently, we revealed a strong prognostic significance of epigenetic silencing of *TUSC3* on survival of ovarian cancer patients (9), however, the molecular mechanism of tumor-suppressor effect of *TUSC3* on cancer cells remained unclear. *TUSC3* deletions or mutations are frequently associated with familial mental retardation syndromes (10,11). *TUSC3* function in regulation of magnesium transport and embryonic development in vertebrates has been suggested (12). *TUSC3* shares a high sequence homology with Ost3p, a subunit of the oligosaccharyltransferase (OST) complex involved in N-glycosylation of proteins in *Saccharomyces cerevisiae* (13-15), implying an analogous function in mammalian cells. Alterations of protein N-glycosylation are associated with carcinogenic properties, such as invasion and metastasis (16-18). Deregulated enzymatic activities of proteins directly involved in N-glycosylation, or the availability of potential glycosylation sites determined by the branching of N-glycans are considered to be crucial for these effects (19-21). Well known targets for differential N-glycosylation in tumor cells or their microenvironment are, among others, growth factor receptors (21,22), immunomodulators (23) or extracellular matrix receptors, such as integrins (24).

In this study, we investigated the subcellular localization of *TUSC3* in human ovarian cancer cell lines and identified it as a binding partner of STT3A, a core protein of oligo-

Correspondence to: Dr Michael Krainer, Department of Internal Medicine I and Comprehensive Cancer Center, Medical University of Vienna, Währinger Gürtel 18-20, A-1090 Vienna, Austria
E-mail: michael.krainer@meduniwien.ac.at

*Contributed equally

Key words: *TUSC3*, ovarian cancer, glycosylation, proliferation

saccharyltransferase complex in endoplasmic reticulum *in vitro*. Additionally, we observed that silencing of *TUSC3* expression *in vitro* stimulates migration and proliferation of ovarian cancer cell lines, in particular under conditions of growth factor deprivation. Taken together, we present the first experimental evidence that a protein involved in N-glycosylation may act as a clinically-relevant tumor suppressor gene in ovarian cancer.

Materials and methods

Cell culture and lentiviral transduction. The cancer cell lines were obtained from American Type Culture Collection and cultured in medium (HEK293T, H134, DMEM; OVCAR-3, α -MEM; SKOV3, McCoy's 5A; TR-170, RPMI-1640) enriched with 10% FCS (fetal calf serum), 50 U/ml penicillin G and 50 μ g/ml streptomycin sulfate at 37°C in a humidified atmosphere with 5% CO₂. For the reconstitution of *TUSC3* expression in H134 cell line, the CDS of the IMAGE clone (BC010370 in pDNR-LIB) was cloned into the expression vector pLP-IRESneo. The FLAG peptide was cloned in frame behind the C-terminus of *TUSC3* to form a *TUSC3*-FLAG fusion protein. The empty vector pLP-IRESneo was used as a control. Transfection was performed with Lipofectamine 2000 (Invitrogen), stable clones were selected with G418 (700 μ g/ml). Downregulation of *TUSC3* in SKOV3 and TR-170 cell lines was performed by lentiviral transduction using a 4-plasmid system with pLKO.1 puro vector containing *TUSC3* shRNA or scrambled control (Open Biosystems, Thermo Fisher Scientific) and HEK-293T packaging cell line. To generate stable cell lines, cells were selected in media containing puromycin (3 μ g/ml). Prior to the proliferation, migration and invasion assays, cells were cultivated in the absence of selection antibiotics and the status of *TUSC3* silencing was assessed by qRT-PCR regularly.

RNA isolation, cDNA synthesis and quantitative real-time RT-PCR. Total RNA from cancer cell lines was prepared using the RNeasy Mini kit (Qiagen) and quality/quantity assessed on RNA Nano Chips (Lab-on-a-Chip, Agilent Technologies). cDNA was synthesized from 1 μ g DNase I-digested total RNA using the DuraScript RT-PCR kit (Sigma-Aldrich). Expression was relatively quantified using TaqMan probes specific for *TUSC3*, Hs00185147_m1 and β 2-microglobulin, Hs99999907_m1 (Applied Biosystems) as described elsewhere (8,25) and expressed in relative ratio units. All PCR reactions were performed from at least three independent experiments, and reverse transcriptase-negative and template-negative controls were included.

Proliferation, migration and invasion assays. Proliferation rates were determined in 96-well format using Cell Titer-Blue cell viability assay (Promega) according to the manufacturer's instructions. Migration and invasion abilities were measured using *in vitro* migration (8.0- μ m pore size control chambers) and invasion assays (BD Matrigel™ invasion chambers). Cells that penetrated the membrane were quantified after Calcein dye (BD Bioscience) uptake by fluorescence measurement at 435_{Ex}-538_{Em} nm. Each data point was calculated as mean of three technical replicates. Three independent experiments were

performed. For direct assessment of cell migration a wound healing assay in a confluent cell monolayer was performed. Wound closure was assessed after 18 h. Representative images out of three independent experiments are shown.

Subcellular fractionation and immunofluorescence. Subcellular fractionation (nuclei, mitochondria, lysosomes, microsomes, and cytoplasm) of H134-*TUSC3*-Flag cells were performed based on a differential centrifugation protocol (1,000, 9,700, 20,200 and 182,000 g_{max} for aforementioned organelles, respectively (26) after cell lysis with a Potter pestle. The purity of these fractions was analyzed by immunoblotting with antibodies against marker proteins for the respective fractions (nucleus, nucleoporin p62; mitochondria, cox 5a; lysosomes, none; microsomes, ribophorin I; and cytoplasm, β -actin; Sigma-Aldrich). A mouse monoclonal anti-FLAG M2 antibody (F3165, Sigma-Aldrich) primary antibody against FLAG and a goat secondary anti-mouse HRP-linked antibody (Calbiochem) were used.

Immunofluorescence staining was performed on formaldehyde-fixed H134-*TUSC3*-FLAG cells with antibodies against FLAG SIG1-25 (F2555, Sigma-Aldrich) and calnexin (polyclonal rabbit antibody, kind gift from E. Ivessa) and counterstained with phalloidin (F-actin). For a morphological overview, the whole cells were stained with hematoxylin/eosin or phalloidin (F-actin)/DAPI (nuclei).

Immunocytochemistry. For immunocytochemical staining, cells on Lab-Tek™ Chamber Slides™ (Nalge Nunc International, Rochester, NY) were formaldehyde-fixed and permeabilized with 0.5% Triton X-100. Endogenous peroxidase activity and slides were blocked with 3% H₂O₂/PBS and 0.2% fish gelatine, respectively. After incubation with polyclonal goat anti-integrin β 1 antibody (1:500, R&D, Minneapolis, MN) and biotinylated rabbit anti-goat antibody (1:200, Vector Laboratories, Burlingame, CA) or with the biotinylated sialic acid-specific lectin SNA (1:200, Vector Laboratories), the streptavidin ABCComplex-HRP (ABC-kit from Dako, Glostrup, Denmark) was employed and subsequently DAB⁺ (Dako) staining was performed. IgG-negative controls were included. Finally, cells were counterstained with hematoxyline/eosin and mounted in Eukitt (O. Kindler GmbH, Freiburg, Germany). Microscopy was performed on an Olympus BX50 upright light microscope (Olympus Europe, Hamburg, Germany) equipped with the Soft Imaging system CC12.

Western blotting and immunoprecipitation. Harvested cells were washed two times with 1X PBS and resuspended in the NP-40 lysis buffer containing 50 mM Tris-Cl (pH 7.4), 150 mM NaCl, 2 mM EDTA, 1% NP-40, 50 mM NaF and supplemented with phosphatase inhibitor cocktail (PhosStop, Roche) and protease inhibitor cocktail (Complete, Roche). Protein extracts (15 μ g) quantified by BCA protein assay (Pierce, Austria), were mixed with 2X Laemmli sample buffer (100 mM Tris pH 6.8, 4% SDS, 200 mM DTT, 20% glycerol and 0.1% bromophenol blue) boiled for 3 min and resolved by 10% sodium dodecyl-sulfate-polycrylamide gel electrophoresis (SDS-PAGE). For analysis of glycosylation of integrin β 1, the 7% SDS-PAGE was employed. The resolved proteins were then electroblotted to the 0.45- μ m PVDF membrane (Millipore) and incubated

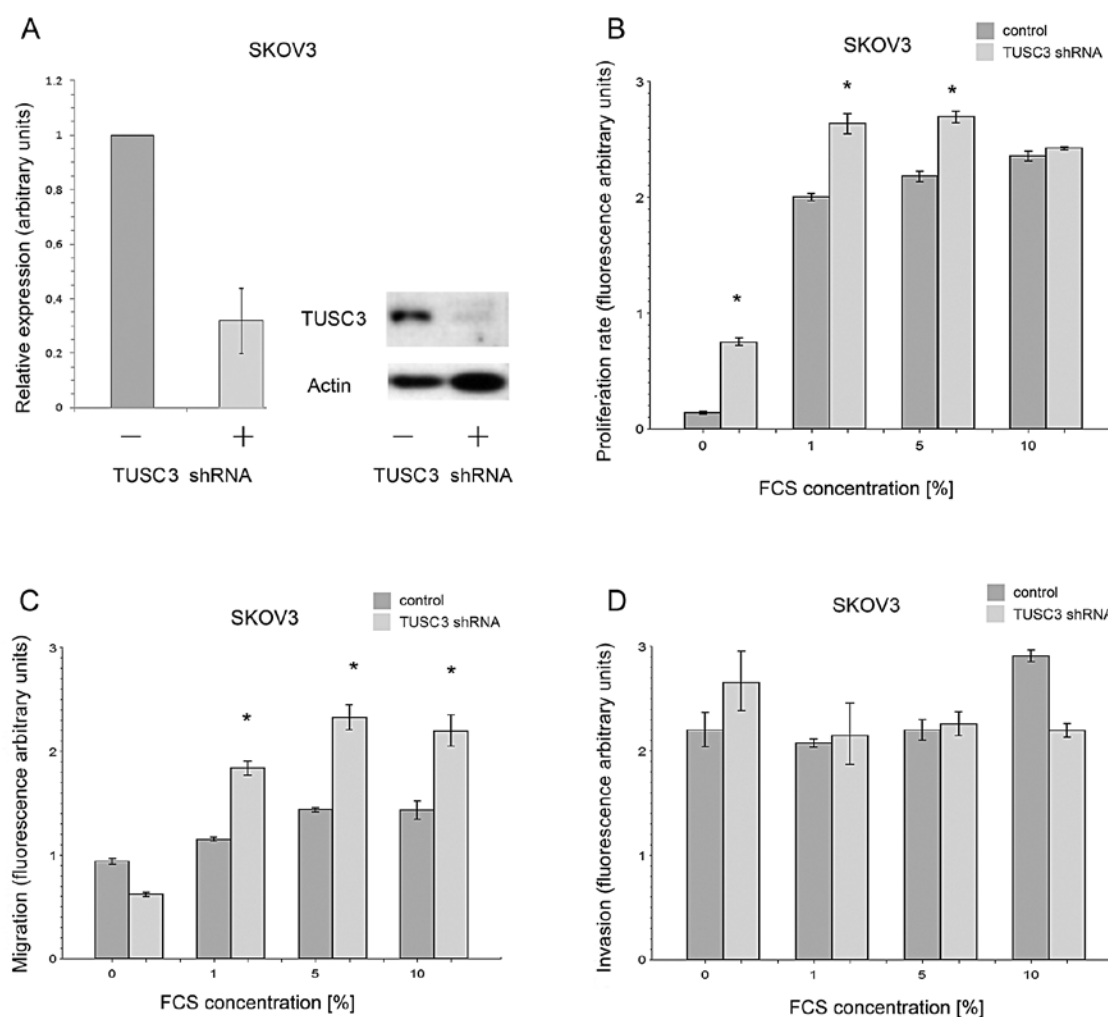


Figure 1. (A) Downregulation of TUSC3 in SKOV-3 cells. β 2-microglobulin-normalized expression of TUSC3 was determined by qRT-PCR and western blotting. (B) Silencing of TUSC3 stimulates metabolic activity/proliferation of SKOV-3 under conditions of serum deprivation. TUSC3-silenced and control SKOV-3 cells were cultivated in 96-well plate for 72 h in a medium supplemented with different concentration of FCS. Accumulation of fluorescent product (Cell Titer-Blue[®] cell viability assay) was then determined. Mean \pm SD of three independent experiments. Asterisks indicate statistical significance at $p \leq 0.001$. (C) Silencing of TUSC3 enhances migration of SKOV-3 cells through 8.0- μ m membrane. TUSC3-silenced and control SKOV-3 cells were seeded on BD transwell plate and cultivated for 24 h. Cells that penetrated the membrane to lower chamber were incubated with Calcein fluorescent dye and quantified by fluorescence measurement at 435_{Ex}, 538_{Em} nm. Mean \pm SD of three independent experiments. Asterisks indicate statistical significance at $p \leq 0.001$. (D) Silencing of TUSC3 does not enhance invasion of SKOV-3 cells through 8.0- μ m tumor invasion system. Quantity of cells penetrating through Matrigel was determined fluorometrically as described in (C). Mean \pm SD of three independent experiments. Asterisks indicate statistical significance at $p \leq 0.001$.

with the indicated primary antibodies diluted 1:500-1:1,000 at 4°C overnight. The blots were developed using horseradish peroxidase-conjugated secondary antibodies (anti-rabbit HRP no. 7074 (Cell Signaling) anti-mouse HRP Ab50043 (Abcam), both 1:4,000 and Immobilon Western HRP substrate (Millipore) according to the manufacturer's instructions.

For co-immunoprecipitation, 150 μ g of cell extracts were precleared using NP-40-washed G-protein beads (Sigma-Aldrich). Supernatants were incubated with 5 μ l of one of the following antibodies: anti-TUSC3 (Ab65213, Abcam), anti-STT3A (Ab55371, Abcam) or commercially available non-specific mouse or rabbit IgG antibody, at 4°C for 1 h. Then, 25 μ l of NP-40-washed G-proteins were added and incubated overnight at 4°C. Pellets were washed four times in NP-40 buffer and resolved by SDS-PAGE.

Statistical analysis. In order to compare the TUSC3 shRNA silenced ovarian cancer cell lines to controls at the specified

FCS concentrations, two-way ANOVA model with interaction was used. P-values for pairwise *post hoc* comparisons were corrected for multiple testing using the Holm-Bonferroni method. $P \leq 0.05$ were considered to be statistically significant. All calculations were performed using the SPSS software Version 13.0 (SPSS Inc.).

Results

Loss of TUSC3 promotes cell proliferation and migration in vitro. To investigate the tumor suppressive function of TUSC3 in an ovarian cancer model, we silenced the expression of TUSC3 in two serous ovarian cystadenocarcinoma cell lines (SKOV-3, TR-170) using shRNA. Efficiency of the knock-down was confirmed on both mRNA and protein levels (Figs. 1A and 2A). Consequently, we analyzed the effect of TUSC3 silencing on cell proliferation, migration and invasion conditions, however, we did not detect

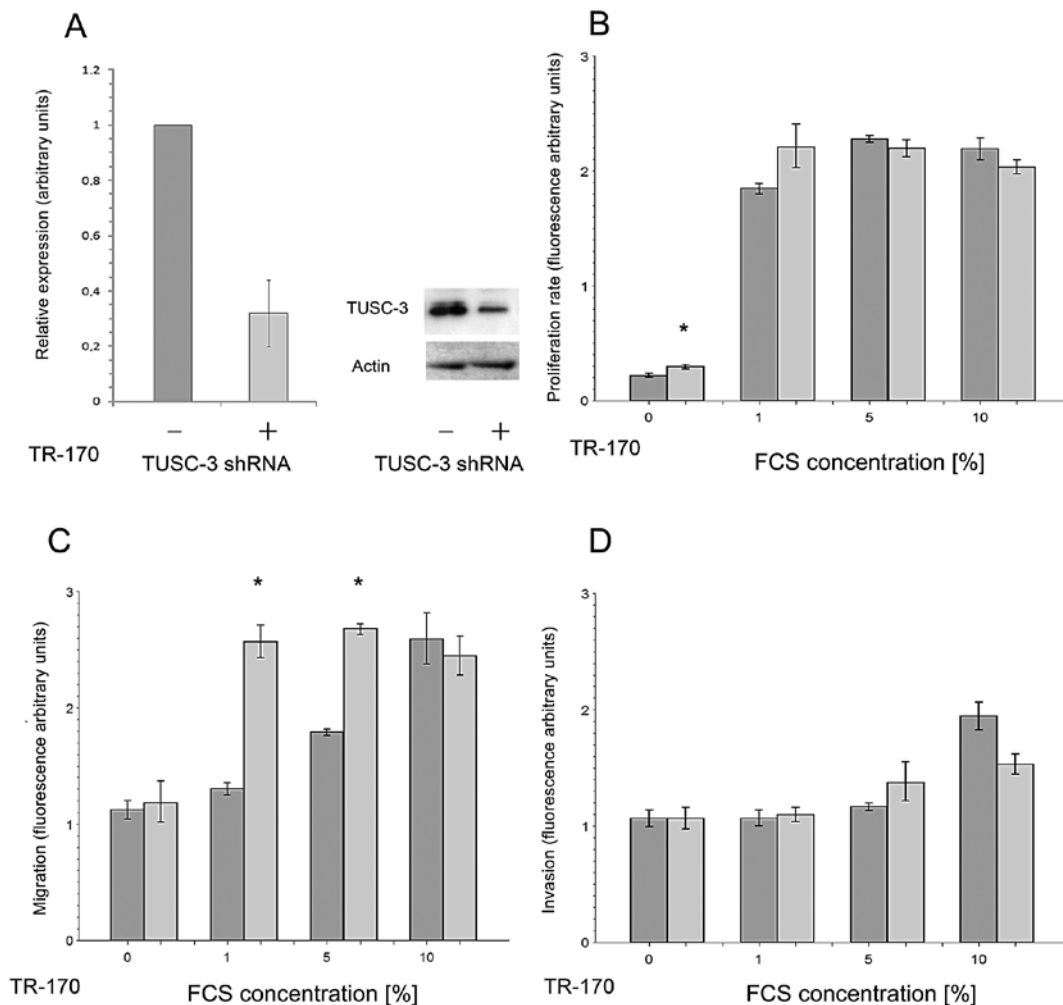


Figure 2. (A) Downregulation of TUSC3 in TR-170 cells. β 2-microglobulin-normalized expression of TUSC3 was determined by qRT-PCR and western blotting. (B) Silencing of TUSC3 stimulates proliferation of TR-170 cells under conditions of serum deprivation. TUSC3-silenced and control TR-170 cells were cultivated for 72 h in a medium supplemented with different concentrations of FCS and quantified as in Fig. 1B. Mean \pm SD of three independent experiments. Asterisks indicate statistical significance at $p \leq 0.001$. (C) Silencing of TUSC3 enhances migration of TR-170 cells through 8.0- μ m membrane. TUSC3-silenced and control TR-170 cells were seeded on BD transwell plate and cultivated for 24 h and quantified as in Fig. 1C. Mean \pm SD of three independent experiments. Asterisks indicate statistical significance at $p \leq 0.001$. (D) Silencing of TUSC3 does not enhance invasion of TR-170 cells through 8.0- μ m tumor invasion system was quantified as in Fig. 1C. Mean \pm SD of three independent experiments.

major differences in proliferation between TUSC3 silenced and control cells cultured under optimal conditions (10% FCS) (Fig. 1B and 2B). To assess their propensity for serum-independent growth, we exposed the cells to stress conditions using varying serum concentrations. Interestingly, the *TUSC3* silenced cells gained a significant survival advantage in contrast to controls after 72 h of cultivation in the absence of serum stimulation (Figs. 1B and 2B). This effect could also be observed to a lesser degree at different time intervals (data not shown). As a next step, we used a Matrigel™ based assay in order to assess effects of TUSC3 knock-down on migration and extracellular matrix (ECM) invasion of ovarian cancer cells. While we did not observe any differences in invasive properties of control ovarian cancer cells regardless of attractant concentration (Figs. 1D and 2D), *TUSC3* silenced cells displayed increased migration through the insert membrane in both cell lines studied (Figs. 1C and 2C). These results were further supported by a wound healing assay, showing increased migration and consequent enhanced closure of the epithelial

monolayer of SKOV-3 cells in no serum or low serum conditions after 18 h (Fig. 3).

TUSC3 is localized in the endoplasmic reticulum as a subunit of the OST complex. The largest part of the data on TUSC3 localization and function is derived from observations of its yeast homologue Ost3p. To determine the subcellular localization of TUSC3 in mammalian cells, we stably transfected the ovarian cancer cell line H134 with a TUSC3-FLAG fusion protein (Fig. 4A). The H134 cell line does not express *TUSC3* due to promoter hypermethylation (data not shown). We performed co-immunofluorescence labeling, which revealed a substantial overlap of the TUSC3-FLAG protein and calnexin, an integral protein of the endoplasmic reticulum (Fig. 4B). Further, subcellular fractions derived from the H134 cells (microsomes, soluble cytoplasm, mitochondria, lysosomes, and nuclei) were analyzed for the presence of exogenous TUSC3-FLAG expression and appropriate fraction markers. We observed TUSC3 enrichment in the microsomal fraction that comprises the endoplasmic

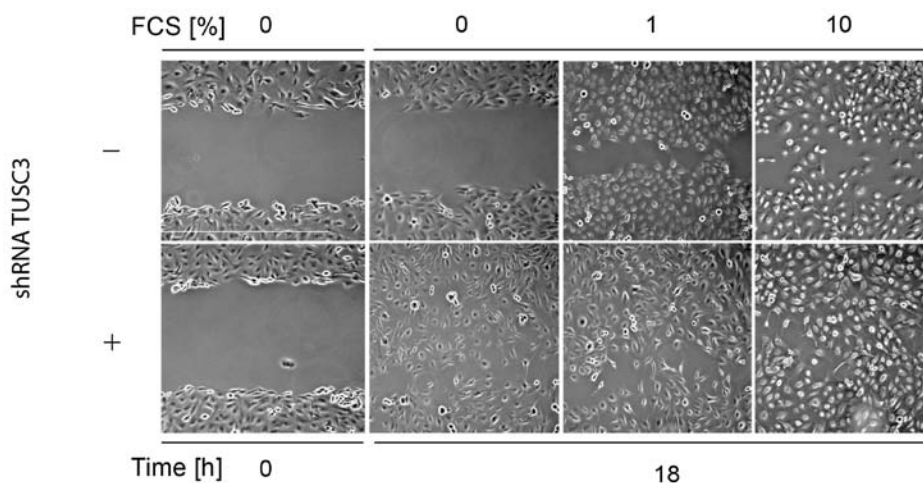


Figure 3. Silencing of TUSC3 stimulates migration of SKOV3 cells. Cells were cultivated at 6-well plates until they reached confluence. The surface was then scratched using sterile tip and cells were cultivated at indicated serum conditions for 18 h. Closing of the gap was assessed by light microscopy. Representative images of three independent experiments are shown.

reticulum (ER) and some minor amounts of cytoplasmic membranes (Fig. 4C). Levels of the endogenous TUSC3 protein in ovarian cancer cell lines were not sufficient for detection in the subcellular fractionation protocol. However, our data confirm the predicted subcellular localization of TUSC3 in the endoplasmic reticulum in ovarian cancer.

Within the endoplasmic reticulum, TUSC3 is supposed to function as a subunit of the OST complex. To determine whether TUSC3 indeed physically interacts with OST in human ovarian cancer cells, we performed co-immunoprecipitation experiments using antibodies specific to endogenous TUSC3 and STT3A, a core catalytic protein of the OST complex. We demonstrated a specific interaction between endogenous TUSC3 and STT3A proteins in TUSC3 expressing ovarian cancer cell lines SKOV-3, TR-170 and OVCAR-3 (Fig. 4D) and provided the evidence for TUSC3 localization in mammalian cells.

TUSC3 modulates glycosylation pattern in H134 ovarian cancer cell line. Next, we wanted to investigate whether there is a causative link between TUSC3 and glycosylation of putative molecular targets. As a model molecule we chose integrin $\beta 1$, a highly glycosylated membrane protein involved in cell adhesion and migration. We employed the H134 with almost null endogenous *TUSC3* gene expression and compared it with H134 cell line highly producing exogenous TUSC3 protein. Probing for integrin $\beta 1$ in H134 total cell extracts on 6% SDS-PAGE revealed bands between 110-150 kDa corresponding to glycosylated integrin $\beta 1$. As a control, a complete removal of N-glycosylated oligosaccharides was achieved by digestion with PNGase F, resulting in bands of equal mobility at ~80 kDa, consistent with the calculated molecular weight of roughly 85 kDa. Interestingly, H134 cells overexpressing TUSC3 showed a shift in bands intensity towards the higher molecular weight when compared to control H134 cells (Fig. 5). Accordingly, immunohistochemical staining of H134 cells for total sialylated proteins using the Sambucus nigra lectin (SNA) revealed an increase in sialylation in TUSC3-positive cells compared to TUSC3-negative cells (Fig. 6). Staining for integrin $\beta 1$ was used as a control.

Discussion

We previously identified *TUSC3* as a candidate tumor suppressor gene in ovarian cancer by systematically screening the chromosomal region 8p22 for differentially regulated genes (8). Nevertheless, mutational analysis performed in several tumor entities failed to reveal a significant rate of protein disruptive mutations and the interest in *TUSC3* gene consequently vanished. Recently, we documented epigenetic silencing of TUSC3 by promoter hypermethylation in various ovarian cell lines and independent cohorts of ovarian cancer patient samples, revealing a strong prognostic potential on survival and indicating a character of tumor-suppressor gene (9). Upregulation of TUSC3 in pancreatic carcinoma cell line MIA-PACA-2 lacking endogenous expression of TUSC3, decreased binding capacity of TUSC3 overexpressing cells to collagen I and prolonged the doubling time (9). However, molecular information on the role of TUSC3 in ovarian cancer is still insufficient.

TUSC3 is the human homologue to *S. cerevisiae* Ost3p, a non-catalytic subunit of the oligosaccharyltransferase complex (14,15). Analyses of the Ost3p and its yeast paralogue Ost6p (human MagT1/IAP) demonstrated their function in regulating glycosylation efficiency (27) and later also uncovered their oxidoreductase activity as well as a possible role in magnesium transport (12). Aberrant glycosylation of proteins can be found in essentially all *in vitro* cancer models and human cancers, and many glycosylated epitopes constitute tumor-associated antigens (28,29), sustaining a long-standing debate if and how protein glycosylation is involved in tumorigenesis. Recently, global DNA methylation changes in ovarian cancer cells were linked to significant alterations of protein glycosylation (30). Re-expression of epigenetically silenced glycosylation enzymes or their subunits, such as TUSC3, may provide a possible explanation for this effect. Our functional analysis builds upon this hypothesis and adds crucial data to the incremental understanding of the causal connection between TUSC3 expression and cancer. We were able to show the subcellular localization of TUSC3 in the endoplasmic

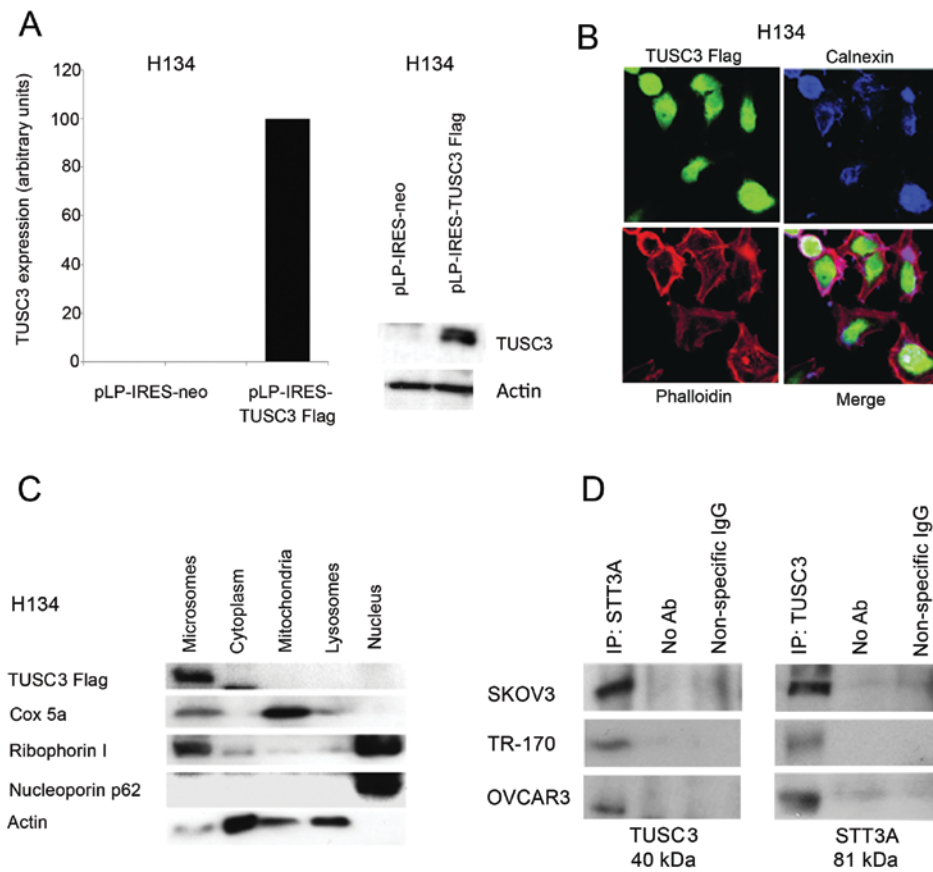


Figure 4. (A) *TUSC3* expression in H134 cell line. H134 cells were transfected with pLP-IRESneo or pLP-IRES-TUSC3-FLAG vectors or left untreated. Transfection was confirmed by *TUSC3*-specific qRT-PCR normalized to $\beta 2$ -microglobulin and western blotting. (B) *TUSC3* colocalizes with endoplasmic reticulum marker calnexin. Colocalization experiment of fixed H134 cells stained with the *TUSC3*-FLAG fusion protein with anti-FLAG antibody, with anti-calnexin for an integral endoplasmic reticulum protein and with phalloidin as a counterstain. (C) Western blot analysis of subcellular fractions for FLAG-tagged *TUSC3* (*TUSC3*-FLAG) in the ovarian cancer cell line H134. Individual fractions - microsomes, cytoplasm, mitochondria, lysosomes and nuclei - were probed with *TUSC3*-Flag and ribophorin I, β -actin, cox 5a and nucleoporin p62, respectively. (D) *TUSC3* co-immunoprecipitates with STT3A. Total proteins from SKOV-3, TR-170 and OVCAR3 cells were extracted and subjected to the co-immunoprecipitation analysis using antibodies specific against *TUSC3* or STT3A. Non-specific IgG was used as a control. Binding partner was visualized by western blotting specific either against *TUSC3* or STT3A.

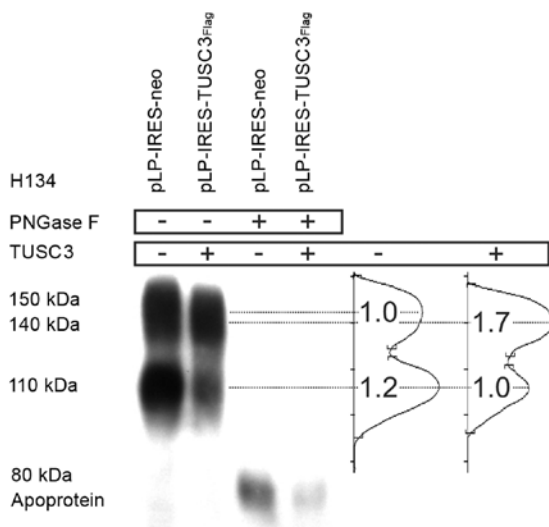


Figure 5. Western blot analysis of integrin $\beta 1$ in H134 cell line. Total cell extracts were resolved on 6% SDS-PAGE, electroblotted to PVDF membrane and probed for integrin $\beta 1$. The 110-kDa band represents the precursor $\beta 1$ -pool in the ER, the 140-150-kDa bands correspond to the mature integrin $\beta 1$ protein. Treatment of proteins with the PNGase F resulted in one band approximately at the position of the calculated apoprotein mass (~80 kDa). Adjacent to the blots, quantification curves and band density ratios according to β -actin are shown. Representative image is shown.

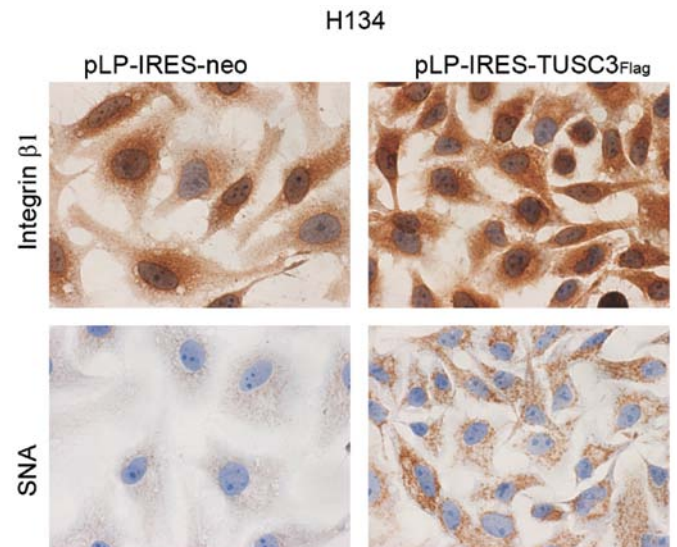


Figure 6. Immunocytochemical stains for sialylated proteins (Sambucus nigra lectin, SNA) and integrin $\beta 1$ in either *TUSC3*-overexpressing or control H134 ovarian cancer model cell line. Cells were formaldehyde-fixed, permeabilized and probed with anti-integrin $\beta 1$ antibody and biotinylated-SNA, respectively. The staining for integrin $\beta 1$ was used as an internal control. Cells were counterstained with hematoxylin/eosin. Representative images are shown.

reticulum of ovarian cancer cells, as predicted from its homology to Ost3p. Further, we demonstrate direct physical interaction between TUSC3 and the OST complex catalytic subunit STT3A. Experiments showing changes in overall or protein-specific glycosylation patterns suggest direct functional involvement of TUSC3 in N-glycosylation. In line with the putative function of TUSC3 as a tumor suppressor, we observed enhanced serum-independent cellular proliferation and migration after silencing of TUSC3 in ovarian cancer cell lines and similarly, a mild increase of the doubling time and reduced migration in H134 cell line overexpressing TUSC3 (data not shown). Although these *in vitro* effects remain relatively modest due to the limitations of a cell culture system, we believe that loss of TUSC3 and consequent aberrant N-glycosylation might have a much greater effect in ovarian cancer progression and metastasis. In light of recent data on N-glycosylation affecting tumor growth in cells with e.g., deregulated PI3K-Akt pathway (22), our results further add to the picture and highlight the possible role of N-glycosylation events in ovarian cancer tumorigenesis.

Taken together, our data are consistent with tumor-suppressive character of TUSC3 published previously (9), but provide the first evidence of a tumor suppressor gene in ovarian cancer involved in protein glycosylation. Although abnormal protein glycosylation is a common event in many cancers, the missing comprehension of its mechanisms and lack of any substantial evidence for causative genetic aberrations are obstructive to development of glycosylation targeted cancer therapies. Defining the molecular function of TUSC3 in ovarian cancer may contribute to understanding the role of N-glycosylation in ovarian cancer and possibly open the door for future drug development.

Acknowledgements

We thank Cornelia Sax, Dr Brigitte Wolf and Andrea Schanzer, for their excellent technical support, Dr Erwin Ivessa for providing the calnexin antibody. This study was supported by the Austrian Science Fund (FWF) grant no. P17891 and Oesterreichische Nationalbank (ONB) grant no. 14109, by the Initiative Krebsforschung and Centre for International Cooperation & Mobility of the Austrian Agency for International Cooperation in Education and Research (project no. CZ 04/2012) and by Ministry of Education, Youth and Sports of Czech Republic (project no. 7AMB12AT019 and CZ.1.07/2.3.00/20.0185).

References

- Jemal A, Bray F, Center MM, Ferlay J, Ward E and Forman D: Global cancer statistics. *CA Cancer J Clin* 61: 69-90, 2011.
- Bova GS, MacGrogan D, Levy A, Pin SS, Bookstein R and Isaacs WB: Physical mapping of chromosome 8p22 markers and their homozygous deletion in a metastatic prostate cancer. *Genomics* 35: 46-54, 1996.
- MacGrogan D, Levy A, Bova GS, Isaacs WB and Bookstein R: Structure and methylation-associated silencing of a gene within a homozygously deleted region of human chromosome band 8p22. *Genomics* 35: 55-65, 1996.
- Bashyam MD, Bair R, Kim YH, *et al*: Array-based comparative genomic hybridization identifies localized DNA amplifications and homozygous deletions in pancreatic cancer. *Neoplasia* 7: 556-562, 2005.
- Levy A, Dang UC and Bookstein R: High-density screen of human tumor cell lines for homozygous deletions of loci on chromosome arm 8p. *Genes Chromosomes Cancer* 24: 42-47, 1999.
- Arbieva ZH, Banerjee K, Kim SY, *et al*: High-resolution physical map and transcript identification of a prostate cancer deletion interval on 8p22. *Genome Res* 10: 244-257, 2000.
- Bova GS, Carter BS, Bussemakers MJ, *et al*: Homozygous deletion and frequent allelic loss of chromosome 8p22 loci in human prostate cancer. *Cancer Res* 53: 3869-3873, 1993.
- Pils D, Horak P, Gleiss A, *et al*: Five genes from chromosomal band 8p22 are significantly down-regulated in ovarian carcinoma: N33 and EFA6R have a potential impact on overall survival. *Cancer* 104: 2417-2429, 2005.
- Pils D, Horak P, Vanhara P, *et al*: Methylation status of TUSC3 is a prognostic factor in ovarian cancer. *Cancer Oct 23, 2012* (Epub ahead of print). doi: 10.1002/cncr.27850.
- Garshasbi M, Hadavi V, Habibi H, *et al*: A defect in the TUSC3 gene is associated with autosomal recessive mental retardation. *Am J Hum Genet* 82: 1158-1164, 2008.
- Molinari F, Foulquier F, Tarpey PS, *et al*: Oligosaccharyltransferase-subunit mutations in nonsyndromic mental retardation. *Am J Hum Genet* 82: 1150-1157, 2008.
- Zhou H and Clapham DE: Mammalian MagT1 and TUSC3 are required for cellular magnesium uptake and vertebrate embryonic development. *Proc Natl Acad Sci USA* 106: 15750-15755, 2009.
- Kelleher DJ and Gilmore R: An evolving view of the eukaryotic oligosaccharyltransferase. *Glycobiology* 16: R47-R62, 2006.
- Kelleher DJ, Karaoglu D, Mandon EC and Gilmore R: Oligosaccharyltransferase isoforms that contain different catalytic STT3 subunits have distinct enzymatic properties. *Mol Cell* 12: 101-111, 2003.
- Schulz BL, Stirnimann CU, Grimshaw JP, *et al*: Oxidoreductase activity of oligosaccharyltransferase subunits Ost3p and Ost6p defines site-specific glycosylation efficiency. *Proc Natl Acad Sci USA* 106: 11061-11066, 2009.
- Collard JG, Schijven JF, Bikker A, La Riviere G, Bolscher JG and Roos E: Cell surface sialic acid and the invasive and metastatic potential of T-cell hybridomas. *Cancer Res* 46: 3521-3527, 1986.
- Dennis JW, Granovsky M and Warren CE: Glycoprotein glycosylation and cancer progression. *Biochim Biophys Acta* 1473: 21-34, 1999.
- Yogeeswaran G and Salk PL: Metastatic potential is positively correlated with cell surface sialylation of cultured murine tumor cell lines. *Science* 212: 1514-1516, 1981.
- Janik ME, Litynska A and Vereecken P: Cell migration-the role of integrin glycosylation. *Biochim Biophys Acta* 1800: 545-555, 2010.
- Kakugawa Y, Wada T, Yamaguchi K, *et al*: Up-regulation of plasma membrane-associated ganglioside sialidase (Neu3) in human colon cancer and its involvement in apoptosis suppression. *Proc Natl Acad Sci USA* 99: 10718-10723, 2002.
- Lau KS, Partridge EA, Grigorian A, *et al*: Complex N-glycan number and degree of branching cooperate to regulate cell proliferation and differentiation. *Cell* 129: 123-134, 2007.
- Fang M, Shen Z, Huang S, *et al*: The ER UDPase ENTPD5 promotes protein N-glycosylation, the Warburg effect, and proliferation in the PTEN pathway. *Cell* 143: 711-724, 2010.
- Kuball J, Hauptrock B, Malina V, *et al*: Increasing functional avidity of TCR-redirected T cells by removing defined N-glycosylation sites in the TCR constant domain. *J Exp Med* 206: 463-475, 2009.
- Seales EC, Jurado GA, Singhal A and Bellis SL: Ras oncogene directs expression of a differentially sialylated, functionally altered beta1 integrin. *Oncogene* 22: 7137-7145, 2003.
- Pfaffl MW: A new mathematical model for relative quantification in real-time RT-PCR. *Nucleic Acids Res* 29: e45, 2001.
- Graham J and Rickwood D (eds): *Subcellular fractionation, a practical approach*. Oxford University Press, New York, 1997.
- Karaoglu D, Kelleher DJ and Gilmore R: Functional characterization of Ost3p. Loss of the 34-kD subunit of the *Saccharomyces cerevisiae* oligosaccharyltransferase results in biased underglycosylation of acceptor substrates. *J Cell Biol* 130: 567-577, 1995.
- Hakomori S: Glycosylation defining cancer malignancy: new wine in an old bottle. *Proc Natl Acad Sci USA* 99: 10231-10233, 2002.
- Kobata A and Amano J: Altered glycosylation of proteins produced by malignant cells, and application for the diagnosis and immunotherapy of tumours. *Immunol Cell Biol* 83: 429-439, 2005.
- Saldova R, Dempsey E, Perez-Garay M, *et al*: 5-AZA-2'-deoxycytidine induced demethylation influences N-glycosylation of secreted glycoproteins in ovarian cancer. *Epigenetics* 6: 1362-1372, 2011.